

# Design of Dual-Band Bandpass Filter Using DGS With Controllable Second Passband

Girdhari Chaudhary, *Student Member, IEEE*, Heungjae Choi, *Member, IEEE*,  
Yongchae Jeong, *Senior Member, IEEE*, Jongsik Lim, *Senior Member, IEEE*, Dongsu Kim, *Member, IEEE*, and  
Jun-Chul Kim, *Member, IEEE*

**Abstract**—In this letter, the application of a variable characteristic impedance transmission line that can be used to design a dual-band bandpass filter (BPF) is presented. The proposed filter offers a fixed first passband and a controllable second passband. The tuning of the second passband is achieved by varying the characteristic impedance of the shunt open stub of stub loaded resonator (SLR) with the help of a defected ground structure (DGS) transmission line and varactor diodes. In order to validate the theoretical predictions and simulated results, a two stage dual-band BPF with three transmission zeros was implemented and experimentally verified.

**Index Terms**—Bandpass filter (BPF), defected ground structure, dual-band filter, stub loaded resonator.

## I. INTRODUCTION

WITH rapid evolution of various wireless services, the demand of multi-band microwave communication systems capable of adapting multiple wireless communication platforms have greatly increased. The BPFs possessing tunable multi-band characteristics are one of the key components in multi-service wireless communication systems. The stub loaded resonators are widely used in the design of BPFs [1], [2]. Recently, multi-mode resonators, such as stepped impedance resonators (SIRs) [3], and stub loaded open loop resonators [4], [5], have been used in the design of multi-band BPFs. It is also of great importance to design tunable dual-band BPFs. A centrally loaded varactor diode in a half-wavelength resonator [6] and a capacitor loaded SIR [7] was presented in the design of a tunable BPF. However, these techniques are mostly focused on the use of variable reactance elements in order to tune the center frequency of the BPFs.

Transmission lines with modified ground structure such as a photonic band gap and a DGS, have been actively studied and applied successfully in the design of various microwave circuits [8], [9]. In this letter, a novel design of the dual-band BPF with the controllable second passband is presented by utilizing the

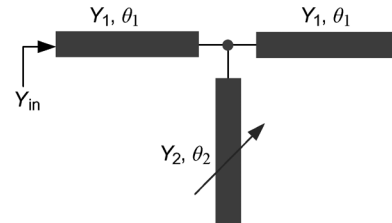


Fig. 1. Structure of tunable stub loaded resonator.

concept of a variable characteristic impedance DGS transmission line.

## II. RESONANT PROPERTIES OF THE RESONATORS AND THE VARIABLE CHARACTERISTIC IMPEDANCE LINE

### A. Stub Loaded Resonator Characteristics

Fig. 1 shows the proposed structure of the tunable SLR, which consists of series resonators and a shunt open stub at the junction point between the series resonators. Assuming  $Y_1, \theta_1$  and  $Y_2, \theta_2$  as the characteristic admittance and electrical length of the series resonators and the shunt open stub, respectively, the input admittance of the proposed structure is given by

$$Y_{in} = jY_1 \frac{2Y_1 \tan \theta_1 + Y_2 \tan \theta_2}{Y_1 - (Y_1 \tan \theta_1 + Y_2 \tan \theta_2) \tan \theta_1}. \quad (1)$$

The resonant condition can be obtained by setting  $Y_{in} = 0$  which is obtained as

$$2Y_1 \tan(a\theta_1) + Y_2 \tan(a\theta_2) = 0 \quad (2)$$

where  $a$  is the ratio of the higher mode resonant frequency ( $f_r$ ) to the fundamental resonant frequency ( $f_1$ ). The fundamental resonant frequency can be obtained from (2) by setting  $a = 1$  and  $\theta_1 = 90^\circ$ . The relationship between the first two resonant frequency ratio ( $a$ ), and the impedance ratio ( $K = Z_2/Z_1$ ) of the SLR is plotted in Fig. 2 using MATLAB. From this figure, it is clear that while keeping the electrical length of the shunt open stub fixed, the frequency ratio can be tuned by varying the impedance ratio,  $K$  of the SLR. This SLR characteristic is applied in the design of the dual-band BPF with the controllable second passband.

### B. Variable Characteristic Impedance Transmission Line

The key idea of this letter is to apply the variable characteristic impedance transmission line to design the dual-band BPF. Fig. 3 shows the structure of the variable characteristic impedance transmission line which consists of a conventional microstrip signal line, the DGS ground island and varactor

Manuscript received June 16, 2011; revised August 05, 2011; accepted August 20, 2011. Date of publication October 06, 2011; date of current version November 09, 2011.

G. Chaudhary and Y. Jeong are with the Department of Electronics and Information Engineering, IT Convergence Research Center, Chonbuk National University, Chollabuk-do 561-756, Korea (e-mail: ycjeong@jbnu.ac.kr).

H. Choi is with Cardiff University, Cardiff CF24 3AA, U.K.

J. Lim is with Soonchunhyang University, Chungcheongnam-do 336-745, Korea.

D. Kim and J.-C. Kim are with Korea Electronics Technology Institute, Gyeonggi 463-816, Korea.

Color versions of one or more of the figures in this letter are available online at <http://ieeexplore.ieee.org>.

Digital Object Identifier 10.1109/LMWC.2011.2167140

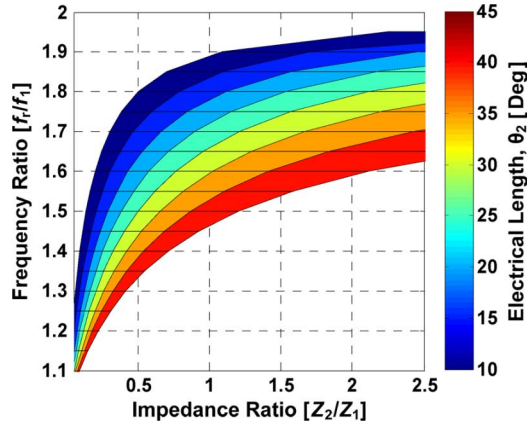


Fig. 2. Dependence of resonant frequency ratio according to characteristic impedance of shunt open stub.

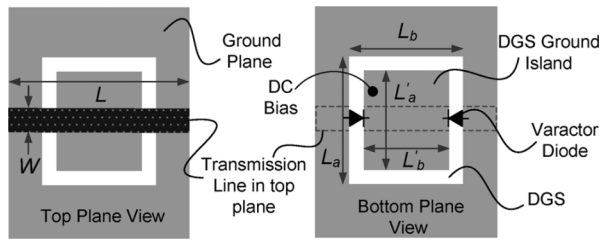


Fig. 3. Variable characteristic impedance transmission line with DGS ground island and varactor diodes ( $L = 11.5$ ,  $L_a = 6$ ,  $L'_a = 6.3$ ,  $L_b = 9.9$ ,  $L'_b = 8.1$ , and  $W = 2.5$  [mm]).

diodes located in the bottom plane of the microstrip line. The varactor diodes are mounted in between the DGS ground island and the ground plane. The characteristic impedance of the modified microstrip line can be tuned as a result of change in the capacitance of the ground plane of the microstrip line with the help of the varactor diodes.

The physical dimensions of the variable characteristic impedance transmission line are shown in Fig. 3, where the substrate is RT/Duroid-5880 of Rogers Corporation with a dielectric constant ( $\epsilon_r$ ) of 2.2 and thickness ( $h$ ) of 31 mils. The characteristic impedance of the transmission line with the modified ground structure can be calculated by applying reflection and transmission theories [10]. Using the method described in [10], the proposed structure has been simulated with HFSS v11 of Ansoft and the calculated characteristic impedance is plotted in Fig. 4. The characteristic impedance ( $Z_c$ ) of this modified line can be varied over 47.5–86  $\Omega$  by changing the capacitance between 20 and 1.5 pF.

To verify the application of variable characteristic impedance line, the full wave electromagnetic (EM) simulation was performed. The two transmission lines with characteristic impedances of 50  $\Omega$  are utilized to feed the proposed SLR using a loose coupling. The dimension of DGS is same as shown in Fig. 3. As seen from Fig. 5, the second resonant frequency can be controlled with help of DGS and varactor diodes in ground plane, whereas the first resonant frequency is preserved.

### III. THE SIMULATION AND EXPERIMENTAL RESULTS

Fig. 6 shows the structure of the proposed dual-band BPF, which consists of SLRs in the signal plane, the DGS ground island and varactor diodes in the ground plane. The microstrip

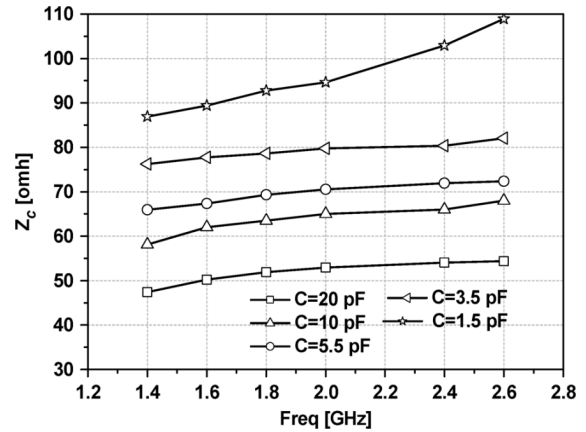


Fig. 4. Calculated characteristic impedances of the proposed variable impedance microstrip line.

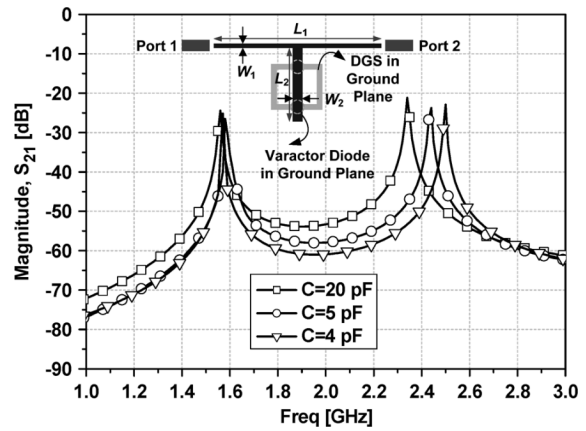


Fig. 5. Resonance frequency of tunable SLR according to capacitance ( $L_1 = 72.5$ ,  $L_2 = 10.8$ ,  $W_1 = 0.65$  and  $W_2 = 2.5$  [mm]).

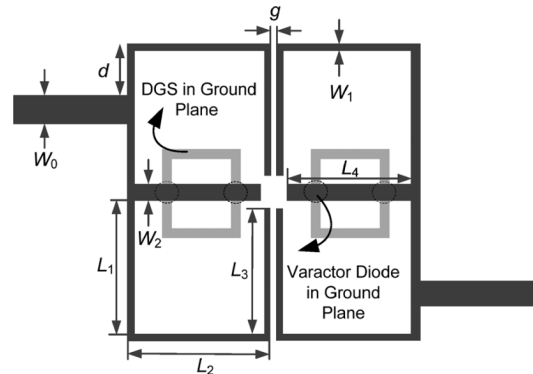


Fig. 6. Proposed dual-band bandpass filter (BPF) in top view ( $L_1 = 10.5$ ,  $L_2 = 13.3$ ,  $L_3 = 11.2$ ,  $L_4 = 10.8$ ,  $W_0 = 2.38$ ,  $W_1 = 0.65$ ,  $W_2 = 2.5$ ,  $d = 3.95$ , and  $g = 0.5$  [mm]).

lines are folded in order to reduce the size, forming open loops. The goal was to design the BPF with constant first passband center frequency of 1.57 GHz and the controllable second passband with initial center frequency of 2.40 GHz. The electrical lengths of  $\theta_1$  and  $\theta_2$  were calculated as  $90^\circ$  and  $30^\circ$  at 1.575 GHz, respectively. The initial characteristic impedances of the SLRs were determined as  $Z_1 = 100 \Omega$  and  $Z_2 = 48 \Omega$ .

The physical dimensions of the proposed filter are shown in Fig. 6. The used varactor diodes were SMV 1234-011LF of Skyworks, whose capacitance range is over 1.4–30 pF according to

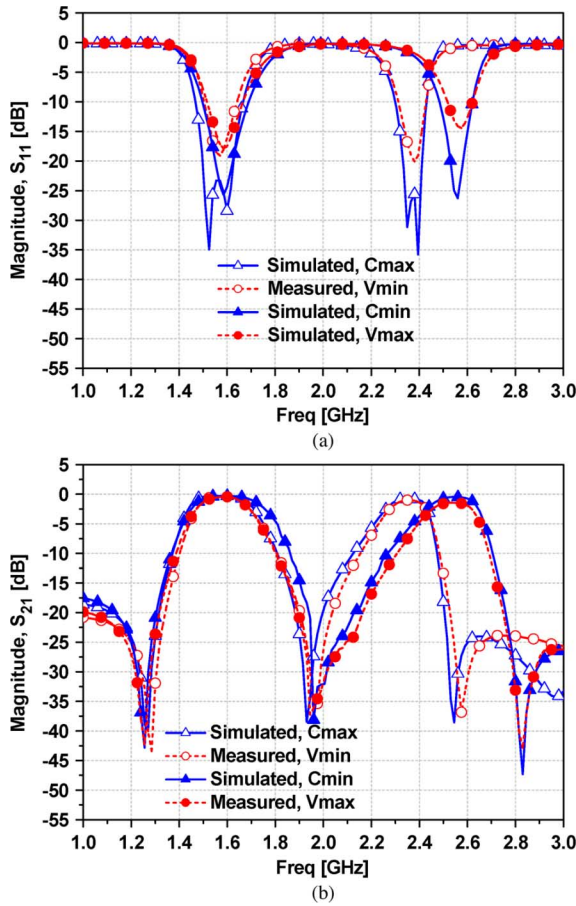


Fig. 7. Simulated and measured results of (a) return loss response and (b) insertion loss response according to varactor diode bias voltage ( $C_{\min} = 1.6$  pF,  $C_{\max} = 30$  pF,  $V_{\min} = 0$  V,  $V_{\max} = 8.2$  V).

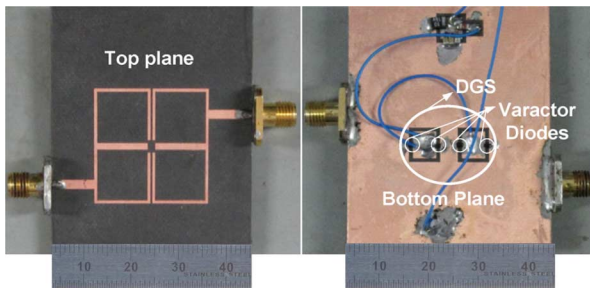


Fig. 8. Photograph of fabricated filter.

the bias range of 15-0 V. However, the varactor diode is considered as ideal variable capacitance in simulation. The simulated and measured results according to the varactor diode bias voltage are plotted in Fig. 7. A close agreement between them can be observed. As described in the previous section, the performance of the first passband remains almost constant. With the central frequency of 1.575 GHz, the first passband has a 3 dB fractional bandwidth of 16.8% and the maximum insertion loss of 0.59 dB.

The measured return loss is less than 18.9 dB at the first passband center frequency. In addition, the second passband center frequency is controllable between 2.38 and 2.56 GHz ( $f_r/f_1 = 1.51 \sim 1.62$  as  $f_1 = 1.575$  GHz). The measured insertion loss varies from 1.112 to 1.438 dB with an almost constant fractional bandwidth of 7.5%. The return loss is less than

14.1 dB at center frequency of the second passband throughout the entire controllable range.

The proposed filter creates three transmission zeros for each bias-voltage. The two transmission zeros generated by two arms (from tapping position to two ends of the open loop as shown in Fig. 5) that correspond to  $90^\circ$  at the frequencies of two transmission zeros around both sides of first passband, are fixed. The remaining transmission zero located on the higher side of the second passband generated as the input impedance viewed from tapping position toward the loaded shunt stub, approaches zeros at frequency of transmission zero, which moves synchronously with the tuning of the second passband due to change in propagation constant of shunt open stub with the help of DGS and varactor diodes on the ground plane. These characteristics of the proposed filter improve the selectivity of the out band frequencies. The photograph of fabricated filter is shown in Fig. 8.

#### IV. CONCLUSION

The novel design of a dual-band BPF with controllable second passband using a variable characteristic impedance transmission line in the stub loaded resonator is presented in this letter. The characteristic impedance of the transmission line can be controlled with the help of the defected ground structure and the varactor diodes located in the ground plane. Both theoretical analysis and experiments were done in order to validate the proposed structure. It was demonstrated that the second passband can be adjusted while keeping the first passband constant. The proposed filter provides low insertion losses throughout the entire tuning range of the second passband which is expected to be applicable to global positioning systems (GPS) and wireless local area networks (WLANs).

#### REFERENCES

- [1] J. R. Lee, J. H. Cho, and S. W. Yun, "New compact bandpass filter using microstrip  $\lambda/4$  resonators with open stub inverter," *IEEE Microw. Guided Wave Lett.*, vol. 10, no. 12, pp. 526–527, Dec. 2000.
- [2] L. Zhu and W. Menzel, "Compact microstrip bandpass filter with two transmission zeros using a stub-tapped half-wavelength line resonator," *IEEE Microw. Wireless Compon. Lett.*, vol. 13, no. 1, pp. 16–18, Jan. 2003.
- [3] Y. P. Zhang and M. Sun, "Dual-band microstrip bandpass filter using stepped impedance resonators with new coupling scheme," *IEEE Trans. Microw. Theory Tech.*, vol. 54, no. 10, pp. 3779–3785, Oct. 2006.
- [4] P. Mondal and M. K. Mandal, "Design of dual-band bandpass filters using stub loaded open loop resonators," *IEEE Trans. Microw. Theory Tech.*, vol. 56, no. 1, pp. 150–155, Jan. 2008.
- [5] X. Y. Zhang, J. X. Chen, Q. Xue, and S. M. Li, "Dual-band bandpass filter using stub-loaded resonators," *IEEE Microw. Wireless Compon. Lett.*, vol. 17, no. 8, pp. 583–585, Aug. 2007.
- [6] X. Y. Zhang and Q. Xue, "Novel centrally loaded resonators and their applications to bandpass filters," *IEEE Trans. Microw. Theory Tech.*, vol. 56, no. 4, pp. 913–921, Apr. 2008.
- [7] D. Girbau, A. Lazaro, E. Martinez, D. Masone, and L. Pradell, "Tunable dual-band bandpass filter for WLAN applications," *Microw. Opt. Tech. Lett.*, vol. 51, no. 9, pp. 2025–2028, Sep. 2009.
- [8] J. Lim, S. Oh, J. Koo, Y. Jeong, and D. Ahn, "A power divider with adjustable dividing ratio," *IEICE Trans. Electron.*, vol. E91-C, no. 3, pp. 389–391, Mar. 2008.
- [9] D. Ahn, J. Park, C. Kim, J. Kim, Y. Qian, and T. Itoh, "A design of the low-pass filter using a novel microstrip defected ground structure," *IEEE Trans. Microw. Theory Tech.*, vol. 49, no. 1, pp. 86–93, Jan. 2001.
- [10] J. Lim, J. Lee, J. Lee, S.-M. Han, D. Ahn, and Y. Jeong, "A new calculation method for the characteristic impedance of transmission lines with modified ground structure or perturbation," *Progress Electrom. Res.*, vol. 106, pp. 147–162, 2010.